

1 LEVERAGING MULTI-MESSENGER ASTROPHYSICS FOR DARK MATTER SEARCHES

By

Daniel Nicholas Salazar-Gallegos

A DISSERTATION

Submitted to
Michigan State University
in partial fulfillment of the requirements
for the degree of

Physics—Doctor of Philosophy
Computational Mathematics in Science and Engineering—Dual Major

Today

ABSTRACT

3 I did Dark Matter with HAWC and IceCube. I also used Graph Neural Networks

⁴ Copyright by

⁵ DANIEL NICHOLAS SALAZAR-GALLEGOS

⁶ Today

ACKNOWLEDGMENTS

8 I love my friends. Thanks to everyone that helped me figure this out. Amazing thanks to the people
9 at LANL who supported me. Eames, etc Dinner Parties Jenny and her child Kaydince Kirsten, Pat,
10 Andrea Family. You're so far but so critical to my formation. Unconditional love. Roommate

TABLE OF CONTENTS

12	LIST OF TABLES	vi
13	LIST OF FIGURES	vii
14	LIST OF ABBREVIATIONS	ix
15	CHAPTER 1 INTRODUCTION	1
16	CHAPTER 2 DARK MATTER IN THE COSMOS	2
17	2.1 Introduction	2
18	2.2 Dark Matter Basics	3
19	2.3 Evidence for Dark Matter	4
20	2.4 Searching for Dark Matter: Particle DM	11
21	2.5 Sources for Indirect Dark Matter Searches	16
22	2.6 Multi-Messenger Dark Matter	18
23	CHAPTER 3 MULTIMESSENGER ASTROPHYSICS: DETECTING HIGH EN-	
24	ERGY NEUTRAL MESSENGERS	22
25	3.1 Introduction	22
26	3.2 Charged Particles in a Medium	22
27	3.3 Photons (γ)	23
28	3.4 Neutrinos (ν)	23
29	3.5 Opportunities to Combine for Dark Matter	23
30	CHAPTER 4 HIGH ALTITUDE WATER CHERENKOV (HAWC) OBSERVATORY .	25
31	4.1 The Detector	25
32	4.2 Events Reconstruction and Data Acquisition	25
33	4.3 Remote Monitoring	25
34	CHAPTER 5 ICECUBE NEUTRINO OBSERVATORY	26
35	5.1 The Detector	26
36	5.2 Events Reconstruction and Data Acquisition	26
37	5.3 Northern Test Site	26
38	CHAPTER 6 COMPUTATIONAL TECHNIQUES IN PARTICLE ASTROPHYSICS .	27
39	6.1 Neural Networks for Gamma/Hadron Separation	27
40	6.2 Parallel Computing for Dark Matter Analyses	27
41	CHAPTER 7 GLORY DUCK	28
42	7.1 Data and Background	28
43	CHAPTER 8 NU DUCK	29
44	BIBLIOGRAPHY	30

45

LIST OF TABLES

46 Proof I know how to include

LIST OF FIGURES

48	Figure 2.1	Rotation curve fit to NGC 6503 from [7]. Dashed line is the contribution 49 from visible matter. Dotted curves are from gas. Dash-dot curves are from 50 dark matter (DM). Solid line is the composite contribution from all matter 51 and DM sources. Data are indicated with bold dots with error bars. Data 52 agree strongly with a matter + DM composite prediction.	5
53	Figure 2.2	Light from distant galaxy is bent in unique ways depending on the distribution 54 of mass between the galaxy and Earth. Yellow dashed lines indicate where 55 the light would have gone if the matter were not present [8].	7
56	Figure 2.3	(left) Optical image of galactic cluster 1E0657-558. (right) X-ray image of the 57 cluster with redder meaning hotter and higher baryon density. (both) Green 58 contours are reconstruction of gravity contours from weak lensing. White 59 rings are the best fit mass maxima at 68.3%, 95.5%, and 99.7% confidence. 60 The matter maxima of the clusters are clearly separated from x-ray maxima. [9]	8
61	Figure 2.4	Plank CMB sky. Sky map features small variations in temperature in primor- 62 dial light. These anisotropies are used to make inferences about the universe's 63 energy budget and developmental history. [10]	9
64	Figure 2.5	Observed Cosmic Microwave Background power spectrum as a function of 65 multipole moment from Plank [10]. Blue line is best fit model from Λ CDM. 66 Red points and lines are data and error, respectively.	10
67	Figure 2.6	Predicted power spectra of CMB for different $\Omega_m h^2$ values for fixed baryon 68 density from [11]. (left) Low $\Omega_m h^2$ increases the prominence of first and 69 second peaks. (middle) $\Omega_m h^2$ is most similar to the observed power spectrum. 70 The second and third peaks are similar in height. (right) $\Omega_m h^2$ is large which 71 suppresses the first peak and raises the prominence of the third peak.	10
72	Figure 2.7	The Standard Model (SM) of particle physics. Figure taken from http://www.quantumdiaries.org/2014/03/14/the-standard-model-a-beautiful-but-flawed-theory/	12
75	Figure 2.8	Simplified Feynman diagram demonstrating with different ways DM can 76 interact with SM particles. The 'X's refer to the DM particles whereas the 77 SM refer to fundamental particles in the SM. The large circle in the center 78 indicates the vertex of interaction and is purposely left vague. The colored 79 arrows refer to different directions of time as well as their respective labels. 80 The arrows indicate the initial and final state of the DM -SM interaction in time.	13

81	Figure 2.9 A single jet event in ATLAS detector from 2017 [16]. Jet momentum was 82 observed to be 1.9 TeV. Missing transverse momentum was observed to be 83 1.9 TeV compared to the initial transverse momentum of the event was 0. 84 Implied MET is traced by a red dashed line in event display.	14
85	Figure 2.10 More detailed pseudo-Feynman diagram of particle cascade from dark matter 86 annihilation into 2 quarks. The quarks hadronize and down to stable particles 87 like γ or the anti-proton (p^-). Diagram pulled from ICRC 2021 presentation 88 on DM annihilation search [17].	15
89	Figure 2.11 Dark Matter (DM) decay spectrum for $b\bar{b}$ initial state and γ final state. Redder 90 spectra are for larger DM masses. Bluer spectra are light DM masses. x is a 91 unitless factor defined as the ratio of the mass of DM, m_χ , and the final state 92 particle energy E_γ . Figure from [19].	17
93	Figure 2.12 Different dark matter density profiles compared. Some models produce ex- 94 ceptionally large densities at small r [20].	18
95	Figure 2.13 The Milky Way Galaxy in photons (γ) and neutrinos (ν) [22]. The Galactic 96 center is at $l=0^\circ$ and is the brightest region in all panels. (top) An Optical 97 color image of the Milky Way galaxy seen from Earth. Clouds of gas and dust 98 obscure some light from stars. (2nd down) Integrated flux of γ -rays observed 99 by the Fermi-LAT telescope [23]. (middle) Expected neutrino emission 100 that corresponds with Fermi-LAT observations. (2nd up) Expected neutrino 101 emission profile after considering detector systematics of IceCube. (bottom) 102 Observed neutrino emission from region of the galactic plane. Substantial 103 neutrino emission was detected.	19
104	Figure 2.14 Dark Matter annihilation spectra for different final state particle and standard 105 model annihilation channels [24]. Photons (red), e^\pm (green), \bar{p} (blue), ν (black).	20
106	Figure 3.1 TODO: Show a nuclear reactor with cherenkov radiation[NEEDS A SOURCE][FACT 107 CHECK THIS]	23
108	Figure 3.2 TODO: absorption spectrum of liquid and solid water[NEEDS A SOURCE][FACT 109 CHECK THIS]	24

LIST OF ABBREVIATIONS

- 111 **MSU** Michigan State University
112 **LANL** Los Alamos National Laboratory
113 **DM** Dark Matter
114 **SM** Standard Model
115 **HAWC** High Altitude Water Cherenkov Observatory

CHAPTER 1

INTRODUCTION

117 Is the text not rendering right? Ah ok it knows im basically drafting the doc still

CHAPTER 2

118

DARK MATTER IN THE COSMOS

119 **2.1 Introduction**

120 The dark matter problem can be summarized in part by the following thought experiment.

121 Let us say you are the teacher for an elementary school classroom. You take them on a field
122 trip to your local science museum and among the exhibits is one for mass and weight. The exhibit
123 has a gigantic scale, and you come up with a fun problem for your class.

124 You ask your class, "What is the total weight of the classroom? Give your best estimation to
125 me in 30 minutes, and then we'll check your guess on the scale. If your guess is within 10% of the
126 right answer, we will stop for ice cream on the way back."

127 The students are ecstatic to hear this, and they get to work. The solution is some variation of
128 the following strategy. The students should give each other their weight or best guess if they do
129 not know. Then, all they must do is add each student's weight and get a grand total for the class.
130 The measurement on the giant scale should show the true weight of the class. When comparing
131 the measured weight to your estimation, multiply the measurement by 1.0 ± 0.1 to get the $\pm 10\%$
132 tolerances for your estimation.

133 Two of your students, Sandra and Mario, return to you with a solution.

134 They say, "We weren't sure of everyone's weight. We used 65 lbs. for the people we didn't
135 know and added everyone who does know. There are 30 of us, and we got 2,000 lbs.! That's a ton!"

136 You estimated 1,900 lbs. assuming the average weight of a student in your class was 60 lbs.
137 So, you are pleased with Sandra's and Mario's answer. You instruct your students to all gather on
138 the giant scale and read off the weight together. To all your surprise, the scale reads *10,000 lbs.!*
139 10,000 is significantly more than a 10% error from 2,000. In fact, it is approximately 5 times more
140 massive than either your or your students' estimates. You think to yourself and conclude there
141 must be something wrong with the scale. You ask an employee to check the scale and verify it is
142 well calibrated. They confirm that the scale is in working order. You weigh a couple of students
143 individually to assess that the scale is well calibrated. Sandra weighs 59 lbs., and Mario weighs

144 62 lbs., typical weights for their age. You then weigh each student individually and see that their
145 weights individually do not deviate greatly from 60 lbs. So, where does all the extra weight come
146 from?

147 This thought experiment serves as an analogy to the Dark Matter problem. The important
148 substitution to make however is to replace the students with stars and the classroom with a galaxy,
149 say the Milky Way. Individually the mass of stars is well measured and defined with the Sun as our
150 nearest test case. However, when we set out to measure the mass of a collection of stars as large as
151 galaxies, our well-motivated estimation is wildly incorrect. There simply is no way to account for
152 this discrepancy except without some unseen, or dark, contribution to mass and matter in galaxies.
153 I set out in my thesis to narrow the possibilities of what this Dark Matter could be.

154 This chapter is organized like the following... **TODO: Text should look like ... Chapter x has**
155 **blah blah blah.**

156 2.2 Dark Matter Basics

157 Presently, a more compelling theory of cosmology that includes Dark Matter (DM) in order
158 to explain a variety of observations is Λ Cold Dark Matter, or Λ CDM. I present the evidence
159 supporting Λ CDM in Section 2.3 yet discuss the conclusions of the Λ CDM model here. According
160 to Λ CDM fit to observations on the Cosmic Microwave Background (CMB), DM is 26.8% of the
161 universe's current energy budget. Baryonic matter, stuff like atoms, gas, and stars, contributes to
162 4.9% of the universe's current energy budget [1, 2, 3].

163 DM is dark; it does not interact readily with light at any wavelength. DM also does not interact
164 noticeably with the other standard model forces (Strong and Weak) at a rate that is readily observed
165 [3]. DM is cold, which is to say that the average velocity of DM is below relativistic speeds [1].
166 'Hot' DM would not likely manifest the dense structures we observe like galaxies, and instead
167 would produce much more diffuse galaxies than what is observed [3, 1]. DM is old; it played a
168 critical role in the formation of the universe and the structures within it [1, 2].

169 Observations of DM have so far been only gravitational. The parameter space available to what
170 DM could be therefore is extremely broad. The broad DM parameter space is iteratively tested in

171 DM searches by supposing a hypothesis that has not yet been ruled out and performing observations
172 to test them. When the observations yield a null result, the parameter space is constrained further.
173 I present some approaches for DM searches in Section 2.4.

174 **2.3 Evidence for Dark Matter**

175 Dark Matter (DM) has been a looming problem in physics for almost 100 years. Anomalies
176 have been observed by astrophysicists in galactic dynamics as early as 1933 when Fritz Zwicky
177 noticed unusually large velocity dispersion in the Coma cluster. Zwicky's measurement was the
178 first recorded to use the Virial theorem to measure the mass fraction of visible and invisible matter
179 in celestial bodies [4]. From Zwicky in [5], "*If this would be confirmed, we would get the surprising*
180 *result that dark matter is present in much greater amount than luminous matter.*" Zwicky's and
181 others' observation did not instigate a crisis in astrophysics because the measurements did not
182 entirely conflict with their understanding of galaxies [4]. In 1978, Rubin, Ford, and Norbert
183 measured rotation curves for ten spiral galaxies [6]. Rubin et al.'s 1978 publication presented a
184 major challenge to the conventional understanding of galaxies that could no longer be dismissed by
185 measurement uncertainties. Evidence has been mounting ever since for this exotic form of matter.
186 The following subsections provide three compelling pieces of evidence in support of the existence
187 of DM.

188 **2.3.1 First Clues: Stellar Velocities**

189 Zwicky, and later Rubin, measured the stellar velocities of various galaxies to estimate their
190 virial mass. The Virial Theorem upon which these observations are interpreted is written as

$$2T + V = 0. \quad (2.1)$$

191 Where T is the kinetic energy and V is the potential energy in a self-gravitating system. The
192 classical Newton's law of gravity from stars and gas was used for gravitational potential modeled in
193 the observed galaxies:

$$V = -\frac{1}{2} \sum_i \sum_{j \neq i} \frac{m_i m_j}{r_{ij}}. \quad (2.2)$$

194 Zwicky et al. measured just the velocities of stars apparent in optical wavelengths [5]. Rubin et al.
 195 added by measuring the velocity of the hydrogen gas via the 21 cm emission line of Hydrogen [6].
 196 The velocities of the stars and gas are used to infer the total mass of galaxies and galaxy clusters
 197 via Equation (2.1). An inferred mass is obtained from the luminosity of the selected sources. The
 198 two inferences are compared to each other as a luminosity to mass ratio which typically yielded [1]

$$\frac{M}{L} \sim 400 \frac{M_{\odot}}{L_{\odot}} \quad (2.3)$$

199 M_{\odot} and L_{\odot} referring to stellar mass and stellar luminosity, respectively. These ratios clearly indicate
 200 a discrepancy in apparent light and mass from stars and gas and their velocities.

201 Rubin et al. [6] demonstrated that the discrepancy was unlikely to be an underestimation of
 202 the mass of the stars and gas. The inferred "dark" mass was up to 5 times more than the luminous
 203 mass. This dark mass also needed to extend well beyond the extent of the luminous matter.

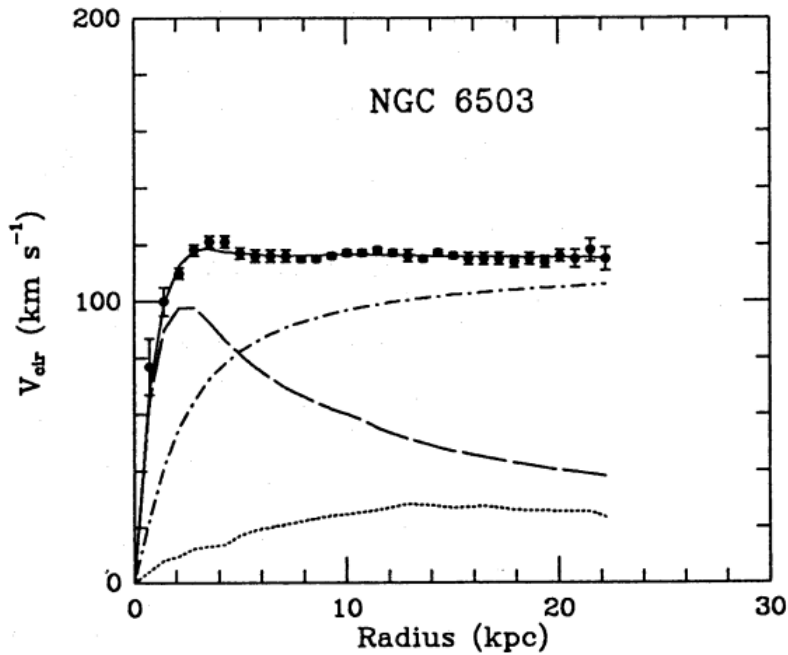


Figure 2.1 Rotation curve fit to NGC 6503 from [7]. Dashed line is the contribution from visible matter. Dotted curves are from gas. Dash-dot curves are from dark matter (DM). Solid line is the composite contribution from all matter and DM sources. Data are indicated with bold dots with error bars. Data agree strongly with a matter + DM composite prediction.

204 Figure 2.1 features one of many rotation curves plotted from the stellar velocities within galaxies.

205 The measured rotation curves mostly feature a flattening of velocities at higher radius which is not
206 expected if the gravity was only coming from gas and luminous matter. The extension of the
207 flat velocity region also indicates that the DM is distributed far from the center of the galaxy.
208 Modern velocity measurements include significantly larger objects, galactic clusters, and smaller
209 objects, dwarf galaxies. Yet, measurements along this regime are leveraging the Virial theorem
210 with Newtonian potential energies. We know Newtonian gravity is not a comprehensive description
211 of gravity. New observational techniques have been developed since 1978, and those are discussed
212 in the following sections.

213 **2.3.2 Evidence for Dark Matter: Gravitational Lensing**

214 Modern evidence for dark matter comes from new avenues beyond stellar velocities. Grav-
215 itational lensing from DM is a new channel from general relativity. General relativity predicts
216 aberrations in light caused by massive objects. In recent decades we have been able to measure the
217 lensing effects from compact objects and DM halos. Figure 2.2 shows how different massive ob-
218 jects change the final image of a faraway galaxy resulting from gravitational lensing. Gravitational
219 lensing developed our understanding of dark matter in two important ways.

220 Gravitational lensing provides additional compelling evidence for DM. The observation of two
221 merging galactic clusters in 2006, shown in Figure 2.3, provided a compelling argument for DM
222 outside the Standard Model. These clusters merged recently in astrophysical time scales. Galaxies
223 and star cluster have mostly passed by each other as the likelihood of their collision is low. Therefore,
224 these massive objects will mostly track the highest mass, dark and/or baryonic, density. Yet, the
225 intergalactic gas is responsible for the majority of the baryonic mass in the systems [4]. These gas
226 bodies will not phase through and will heat up as they collide together. The hot gas is located via
227 x-ray emission from the cluster. Two observations of the clusters were performed independently of
228 each other.

229 The first was the lensing of light around the galaxies due to their gravitational influences.
230 When celestial bodies are large enough, the gravity they exert bends space and time itself. The
231 warped space-time lenses light and will deflect in an analogous way to how glass lenses will bend

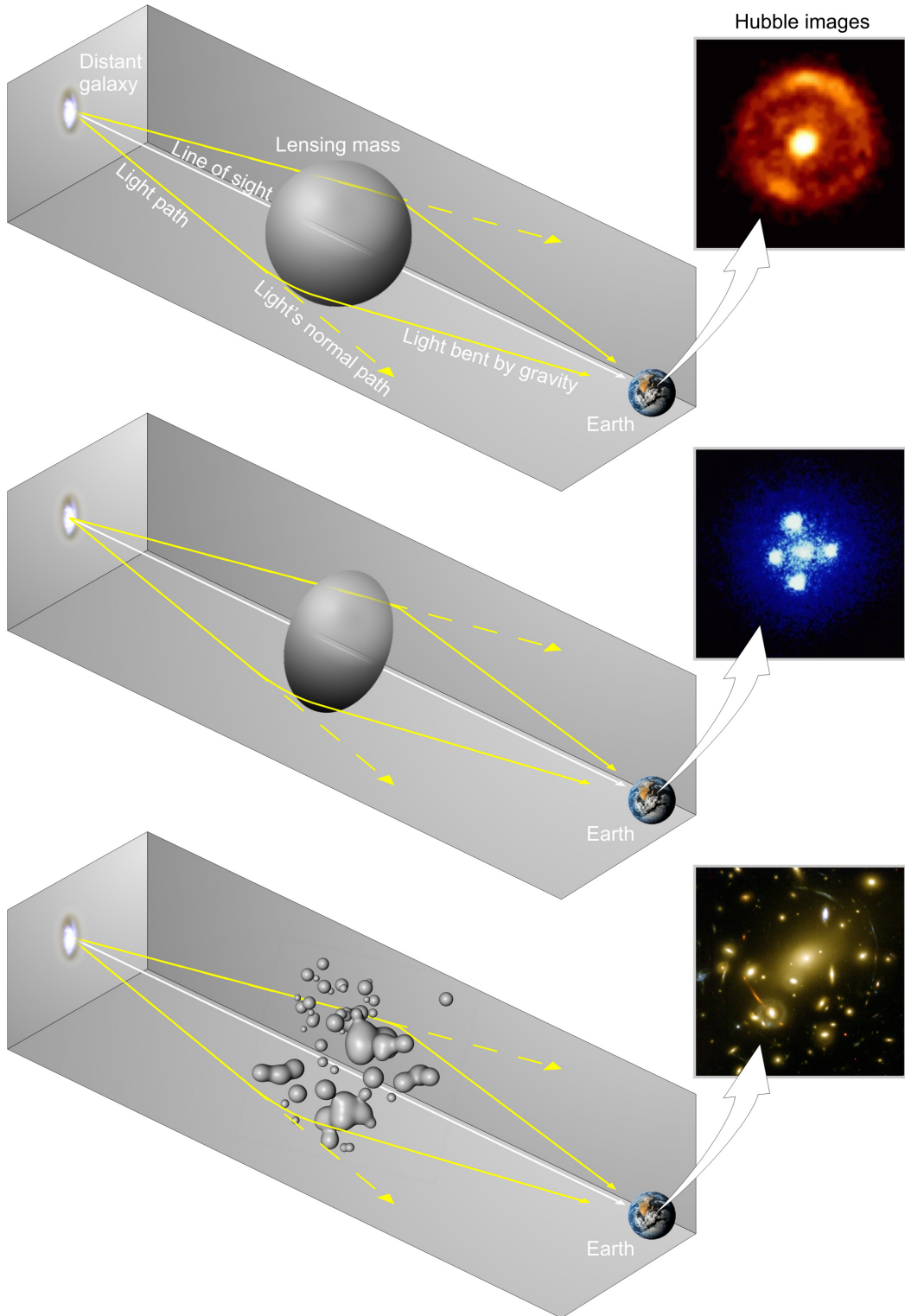


Figure 2.2 Light from distant galaxy is bent in unique ways depending on the distribution of mass between the galaxy and Earth. Yellow dashed lines indicate where the light would have gone if the matter were not present [8].

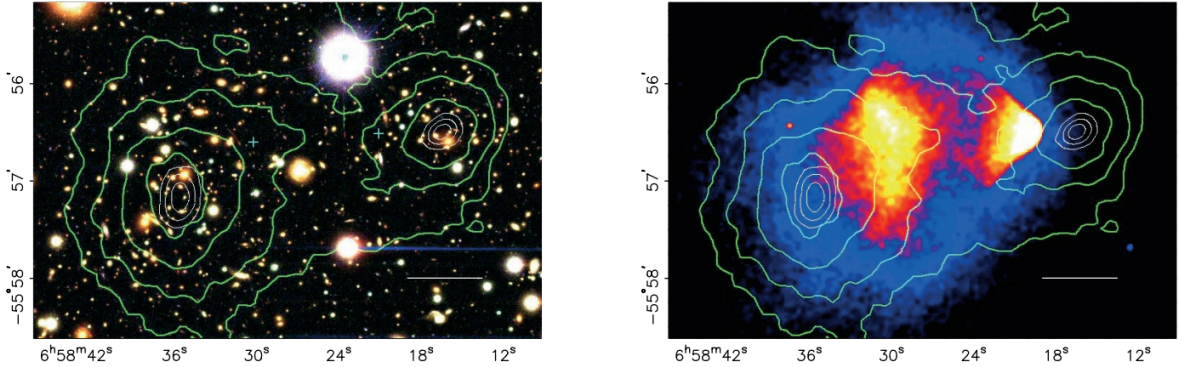


Figure 2.3 (left) Optical image of galactic cluster 1E0657-558. (right) X-ray image of the cluster with redder meaning hotter and higher baryon density. (both) Green contours are reconstruction of gravity contours from weak lensing. White rings are the best fit mass maxima at 68.3%, 95.5%, and 99.7% confidence. The matter maxima of the clusters are clearly separated from x-ray maxima. [9]

232 light, see Figure 2.2. With a sufficient understanding of light sources behind a massive object, we
 233 can reconstruct the contours of the gravitational lenses. The gradient of the contours shown in
 234 Figure 2.3 then indicates how dense the matter is and where it is.

235 The x-ray emission can then be observed from the clusters. Since these galaxies are mostly gas
 236 and are merging, then the gas should be getting hotter. If they are merging, the x-ray emissions
 237 should be the strongest where the gas is mostly moving through each other. Hence, X-ray emission
 238 maps out where the gas is in the merging galaxy cluster.

239 The lensing and x-ray observations were done on the Bullet cluster featured on Figure 2.3.
 240 The x-ray emissions do not align with the gravitational contours from lensing. The incongruence
 241 in mass density and baryon density suggests that there is a lot of matter somewhere that does
 242 not interact with light. Moreover, this dark matter cannot be baryonic [9]. The Bullet Cluster
 243 measurement did not really tell us what DM is exactly, but it did give the clue that DM also does
 244 not interact with itself very strongly. If DM did interact strongly with itself, then it would have been
 245 more aligned with the x-ray emission [9]. There have been follow-up studies of galaxy clusters with
 246 similar results. The Bullet Cluster and others like it provide a persuasive case against something
 247 possibly amiss in our gravitational theories.

248 **2.3.3 Evidence for Dark Matter: Cosmic Microwave Background**

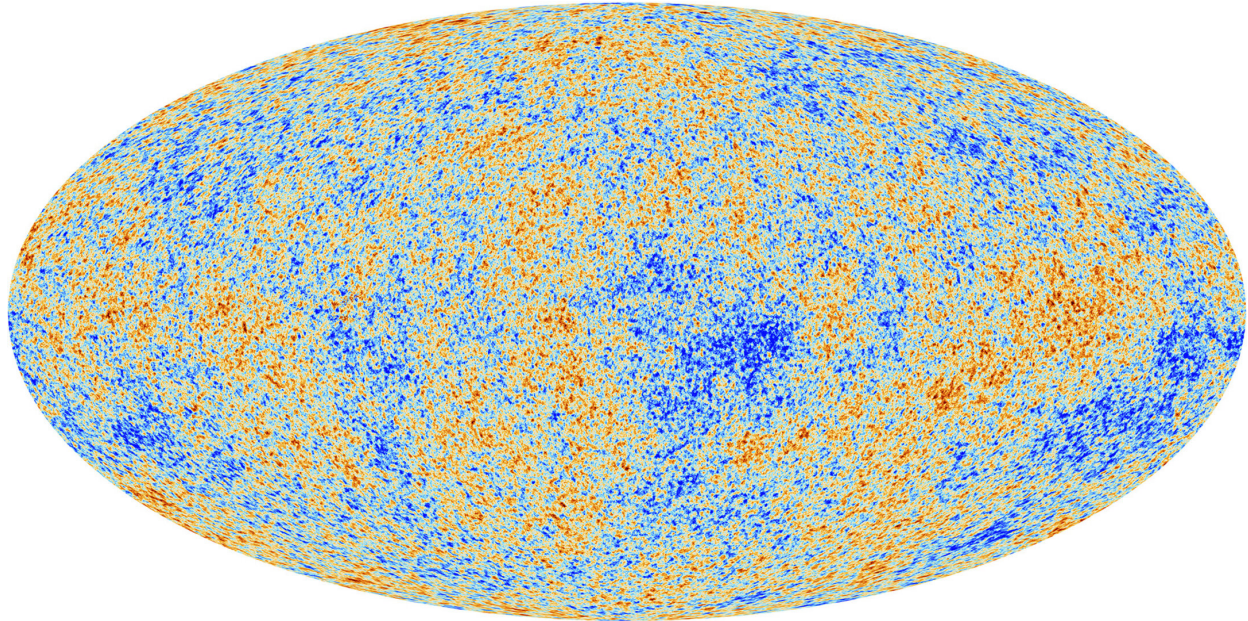


Figure 2.4 Plank CMB sky. Sky map features small variations in temperature in primordial light. These anisotropies are used to make inferences about the universe's energy budget and developmental history. [10]

249 The Cosmic Microwave Background (CMB) is the primordial light from the early universe
250 when Hydrogen atoms formed from the free electron and proton soup in the early universe. The
251 CMB is the earliest light we can observe; released when the universe was about 380,000 years old.
252 Then we look at how the simulated universes look like compared to what we see. Figure 2.4 is the
253 most recent CMB image from the Plank satellite after subtracting the average value and masking the
254 galactic plane [10]. Redder regions indicate a slightly hotter region in the CMB, and blue indicates
255 colder. The intensity variations are on the order of 1 in 1000 with respect to the average value.

256 The Cosmic Microwave Background shows that the universe had DM in it from an incredibly
257 early stage. To measure the DM, Dark Energy, and matter fractions of the universe from the CMB,
258 the image is analyzed into a power spectrum, which shows the amplitude of the fluctuations as
259 a function of spherical multipole moments. Λ CDM provides the best fit to the power spectra of
260 the CMB as shown in Figure 2.5. The CMB power spectrum is quite sensitive to the fraction
261 of each energy contribution in the early universe. Low l modes are dominated by variations

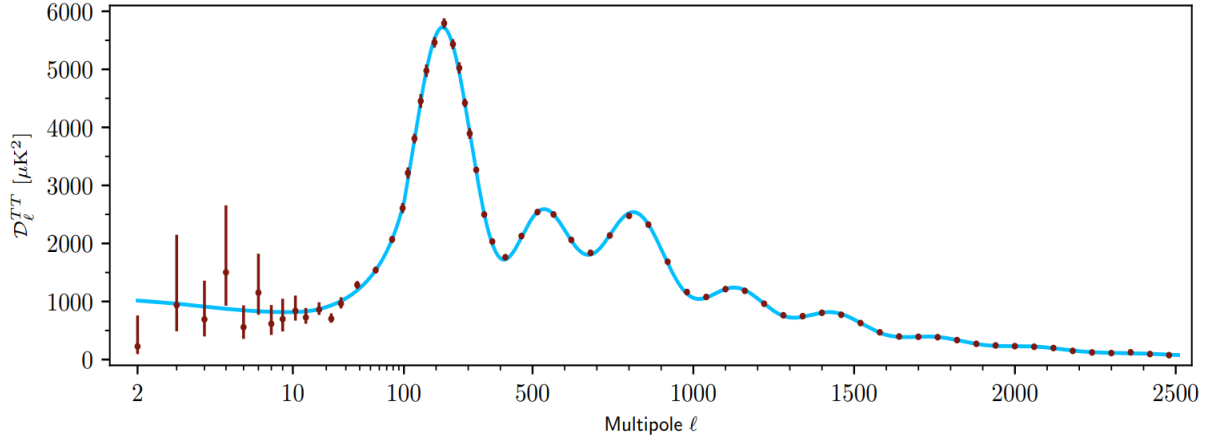


Figure 2.5 Observed Cosmic Microwave Background power spectrum as a function of multipole moment from Plank [10]. Blue line is best fit model from Λ CDM. Red points and lines are data and error, respectively.

in gravitational potential. Intermediate l emerge from oscillations in photon-baryon fluid from competing baryon pressures and gravity. High l is a damped region from the diffusion of photons during electron-proton recombination. [1]

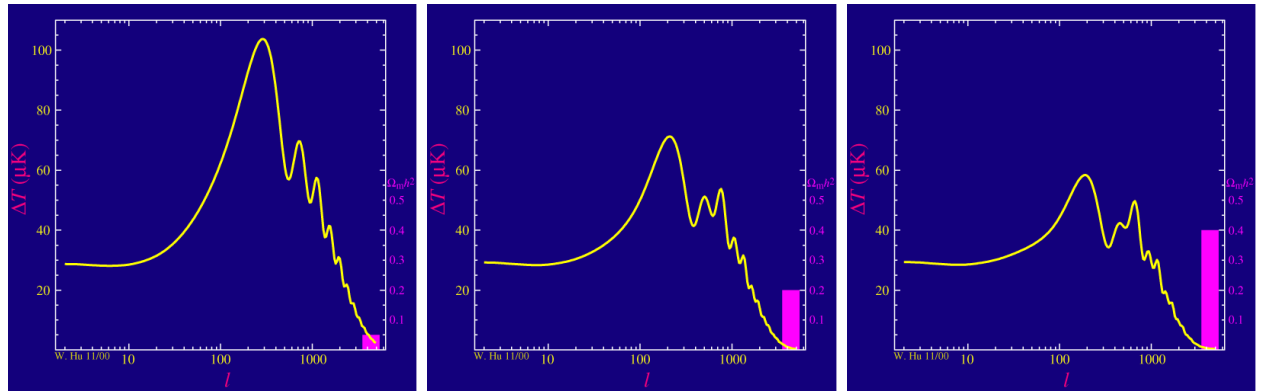


Figure 2.6 Predicted power spectra of CMB for different $\Omega_m h^2$ values for fixed baryon density from [11]. (left) Low $\Omega_m h^2$ increases the prominence of first and second peaks. (middle) $\Omega_m h^2$ is most similar to the observed power spectrum. The second and third peaks are similar in height. (right) $\Omega_m h^2$ is large which suppresses the first peak and raises the prominence of the third peak.

The harmonics would look quite different for a universe with less DM. Figure 2.6 demonstrates the effect $\Omega_m h^2$ has on the expected power spectrum for fixed baryon matter density. [11] Sweeping $\Omega_m h^2$ in this way clearly shows the effect dark matter has on the CMB power spectrum. The observations fit well with the Λ CDM model, and the derived fractions are as follows. The matter

fraction: $\Omega_m = 0.3153$; and the baryon fraction: $\Omega_b = 0.04936$ [10]. Plank's observations also provide a measure of the Hubble constant, H_0 . H_0 especially has seen a growing tension in the past decade that continues to deepened with observations from instruments like the James Webb Telescope [12, 13]. As Hubble tensions deepen, we may find that perhaps ΛCDM , despite its successes, is missing some critical physics.

Overall, the Newtonian motion of stars in galaxies, weak lensing from galactic clusters, and power spectra from primordial light form a compelling body of research in favor of dark matter. It takes another leap of theory and experimentation to make observations of DM that are non-gravitational in nature. In Section 2.3, the evidence for DM implies strongly that the DM is matter and not a lost parameter in the gravitational fields between massive objects. Finally, if we take one axiom: that this matter has quantum behavior, such as being described by some Bohr wavelength and abiding by some fermion or boson statistics; then we arrive at particle dark matter. One particle DM hypothesis is the Weakly Interacting Massive Particle (WIMP). This DM candidate theory is discussed further in the next section and is the focus of this thesis.

2.4 Searching for Dark Matter: Particle DM

Section 2.4 shows the Standard Model of particle physics and is currently the most accurate model for the dynamics of fundamental particles like electrons and photons. The current status of the SM does not have a viable DM candidate. When looking at the standard model, we can immediately exclude any charged particle because charged particles interact strongly with light. Specifically, this will rule out the following charged, fundamental particles: $e, \mu, \tau, W, u, d, s, c, t, b$ and their corresponding antiparticles. Recalling from Section 2.2 that DM must be long-lived and stable over the age of the universe which excludes all SM particles with decay half-lives at or shorter than the age of the universe. The lifetime constraint additionally eliminates the Z and H bosons. Finally, the candidate DM needs to be somewhat massive. Recall from Section 2.2 that DM is cold or not relativistic through the universe. This eliminates the remaining SM particles: $\nu_{e,\mu,\tau}, g, \gamma$ as DM candidates. Because there are no DM candidates within the SM, the DM problem strongly hints to physics beyond the SM (BSM).

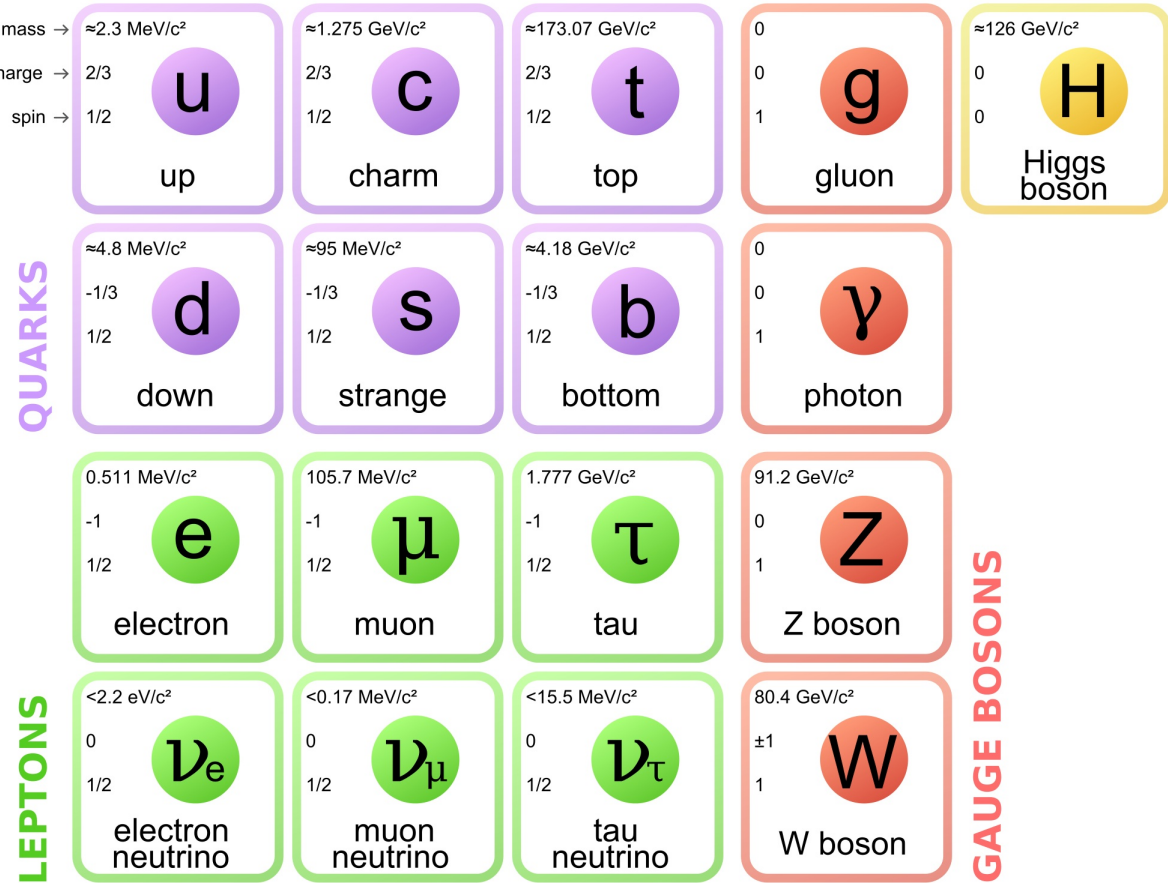


Figure 2.7 The Standard Model (SM) of particle physics. Figure taken from <http://www.quantumdiaries.org/2014/03/14/the-standard-model-a-beautiful-but-flawed-theory/>

296 2.4.1 Shake it, Break it, Make it

297 When considering DM that couples in some way with the SM, the interactions are roughly
 298 demonstrated by interaction demonstrated in Figure 2.8. The figure is a simplified Feynman
 299 diagram where the arrow of time represents the interaction modes of: **Shake it, Break it, Make it.**

300 **Shake it** refers to the direct detection of dark matter. Direct detection interactions start with
 301 a free DM particle and an SM particle. The DM and SM interact via elastic or inelastic collision
 302 and recoil away from each other. The DM remains in the dark sector and imparts some momentum
 303 onto the SM particle. The hope is that the momentum imparted onto the SM particle is sufficiently
 304 high enough to pick up with extremely sensitive instruments. Because we cannot create the DM in
 305 the lab, a direct detection experiment must wait until DM is incident on the detector. Most direct
 306 detection experiments are therefore placed in low-background environments with inert detection

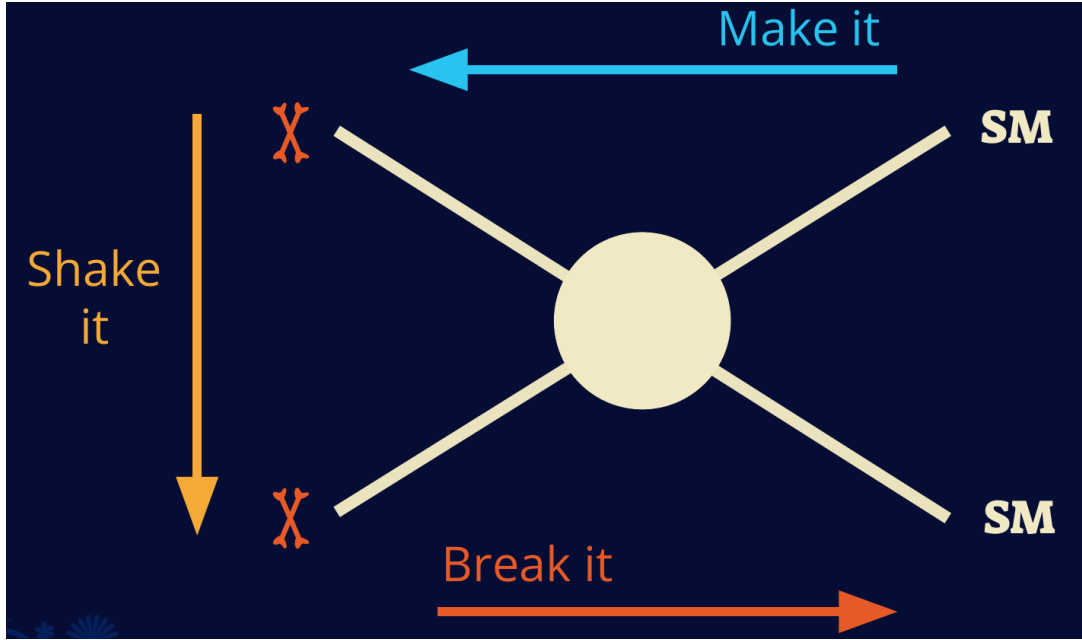


Figure 2.8 Simplified Feynman diagram demonstrating different ways DM can interact with SM particles. The 'X's refer to the DM particles whereas the SM refer to fundamental particles in the SM. The large circle in the center indicates the vertex of interaction and is purposely left vague. The colored arrows refer to different directions of time as well as their respective labels. The arrows indicate the initial and final state of the DM -SM interaction in time.

307 media like the noble gas Xenon. [14]

308 **Make it** refers to the production of DM from SM initial states. The experiment starts with
 309 particles in the SM. These SM particles are accelerated to incredibly high energies and then collide
 310 with each other. In the confluence of energy, DM hopefully emerges as a byproduct of the SM
 311 annihilation. Often it is the collider experiments that are energetic enough to hypothetically produce
 312 DM. These experiments include the world-wide collaborations ATLAS and CMS at CERN where
 313 proton collide together at extreme energies. The DM searches, however, are complex. DM likely
 314 does not interact with the detectors and lives long enough to escape the detection apparatus of
 315 CERN's colliders. This means any DM production experiment searches for an excess of events
 316 with missing momentum or energy in the events. An example event with missing transverse
 317 momentum is shown in Figure 2.9. The missing momentum with no particle tracks implies a
 318 neutral particle carried the energy out of the detector. However, there are other neutral particles
 319 in the SM, like neutrons or neutrinos, so any analysis has to account for SM signatures of missing

320 momentum. [15]

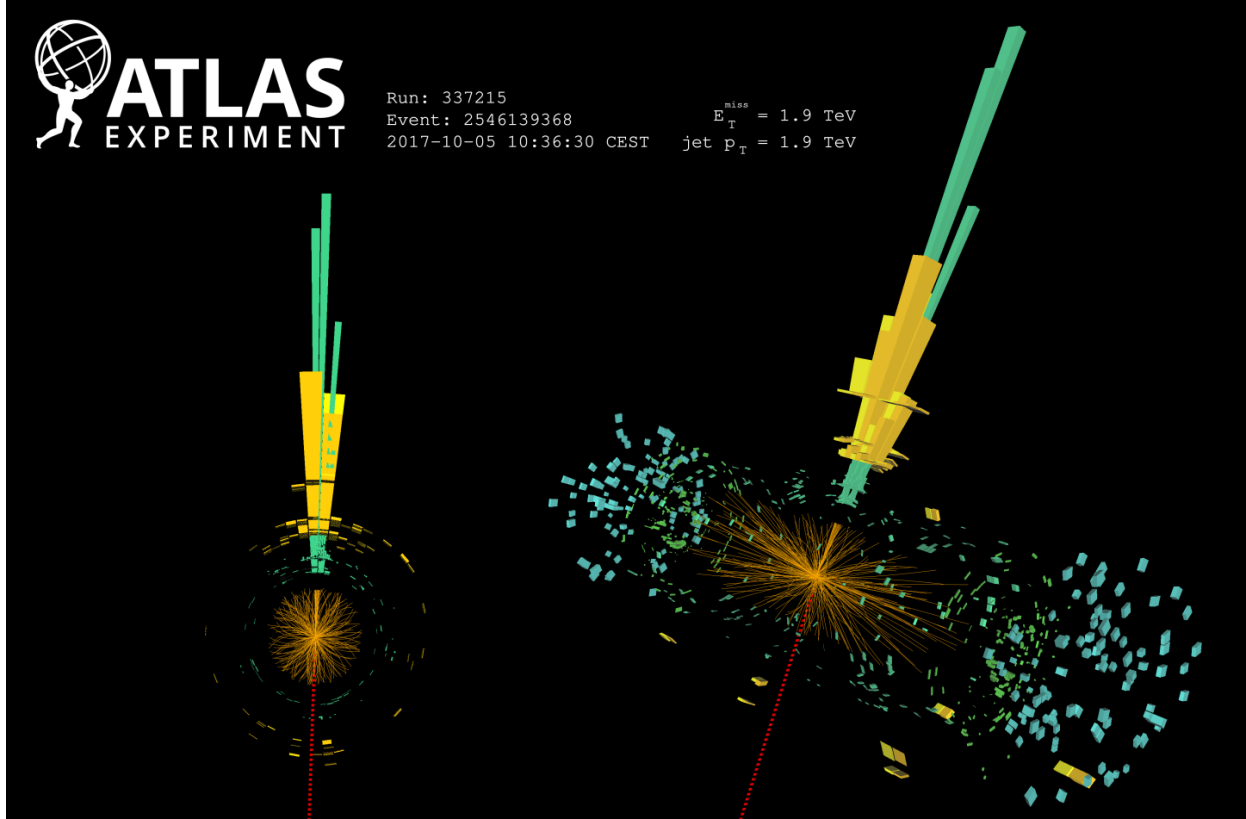


Figure 2.9 A single jet event in ATLAS detector from 2017 [16]. Jet momentum was observed to be 1.9 TeV. Missing transverse momentum was observed to be 1.9 TeV compared to the initial transverse momentum of the event was 0. Implied MET is traced by a red dashed line in event display.

321 2.4.2 Break it: Standard Model Signatures of Dark Matter through Indirect Searches

322 **Break it** refers to the creation of SM particles from the dark sector, and it is the primary focus
323 of this thesis. The interaction begins with DM or in the dark sector. The hypothesis is that this
324 DM will either annihilate with itself or decay and produce an SM byproduct. This method is
325 often referred to as the Indirect Detection of DM because we have no lab to directly control or
326 manipulate the DM. Therefore, most indirect DM searches are performed using observations of
327 known DM densities among the astrophysical sources. The strength is that we have the whole of the
328 universe and its 13.6-billion-year lifespan to use as a detector and particle accelerator. Additionally,
329 locations of dark matter are well cataloged since it was astrophysical observations that presented

330 the problem of DM in the first place.

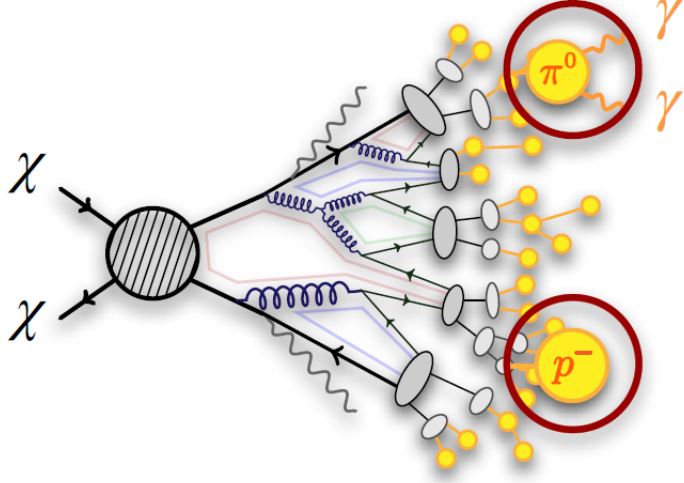


Figure 2.10 More detailed pseudo-Feynman diagram of particle cascade from dark matter annihilation into 2 quarks. The quarks hadronize and down to stable particles like γ or the anti-proton (p^-). Diagram pulled from ICRC 2021 presentation on DM annihilation search [17].

331 However, anything can happen in the universe. There are many difficult to deconvolve back-
332 grounds when searching for DM. One prominent example is the galactic center. We know the
333 galactic center has a large DM content because of stellar kinematics in our Milky Way and DM halo
334 simulations. Yet, any signal from the galactic center is challenging to parse apart from the extreme
335 environment of our supermassive black hole, unresolved sources, and diffuse emission from the
336 interstellar medium [18]. Despite the challenges, any DM model that yields evidence in the other
337 two observation methods, **Shake it or Make it** must be corroborated with indirect observations of
338 the known DM sources. Without corroborating evidence, DM observation in the lab is hard-pressed
339 to demonstrate that it is the model contributing to the DM seen at the universal scale.

340 In the case of WIMP DM, signals are described in terms of primary SM particles produced
341 from DM decay or annihilation. The SM initial state particles are then simulated down to stable
342 final states such as the γ , ν , p , or e which can traverse galactic lengths to reach Earth.

343 Figure 2.10 shows the quagmire of SM particles that emerges from SM initial states that are not

stable [17]. There are many SM particles with varying energies that can be produced in such an interaction. For any arbitrary DM source and stable SM particle, the SM flux from DM annihilating to a neutral particle in the SM, ϕ , from a region in the sky is described by the following.

$$\frac{d\Phi_\phi}{dE_\phi} = \frac{\langle\sigma v\rangle}{8\pi m_\chi^2} \frac{dN_\phi}{dE_\phi} \times \int_{\text{source}} d\Omega \int_{l.o.s} \rho_\chi^2 dl(r, \theta') \quad (2.4)$$

In Equation (2.4), $\langle\sigma v\rangle$ is the velocity-weighted annihilation cross-section of DM to the SM. m_χ refers to the mass of DM, noted with Greek letter χ . $\frac{dN_\phi}{dE_\phi}$ is the N particle flux weighted by the particle energy. An example is provided in Figure 2.11 for the γ final state. The integrated terms are performed over the solid angle, $d\Omega$, and line of sight, l.o.s. ρ is the density of DM for a location (r, θ') in the sky. The terms left of the ' \times ' are often referred to as the particle physics component. The terms on the right are referred to as the astrophysical component. For decaying DM, the equation changes to...

$$\frac{d\Phi_\phi}{dE_\phi} = \frac{1}{4\pi\tau m_\chi} \frac{dN_\phi}{dE_\phi} \times \int_{\text{source}} d\Omega \int_{l.o.s} \rho_\chi dl(r, \theta') \quad (2.5)$$

In Equation (2.5), τ is the decay lifetime of the DM. Just as in Equation (2.4), the left and right terms are the particle physics and the astrophysical components respectively. The integrated astrophysical component of Equation (2.4) is often called the J-Factor. Whereas the integrated astrophysical component of Equation (2.5) is often called the D-Factor.

Exact DM $\text{DM} \rightarrow \text{SM}$ branching ratios are not known, so it is usually assumed to go 100% into an SM particle/anti-particle. Additionally, when a DM annihilation or decay produces one of the neutral, long-lived SM particles (ν or γ), the particle is traced back to a DM source. For DM above GeV energies, there are very few SM processes that can produce particles with such a high energy. Seeing such a signal would almost certainly be an indication of the presence of dark matter. Fortunately, the universe provides us with the largest volume and lifetime ever for a particle physics experiment.

2.5 Sources for Indirect Dark Matter Searches

The first detection of DM relied on optical observations. Since then, we have developed new techniques to find DM dense regions. As described in Section 2.3.1, many DM dense regions were

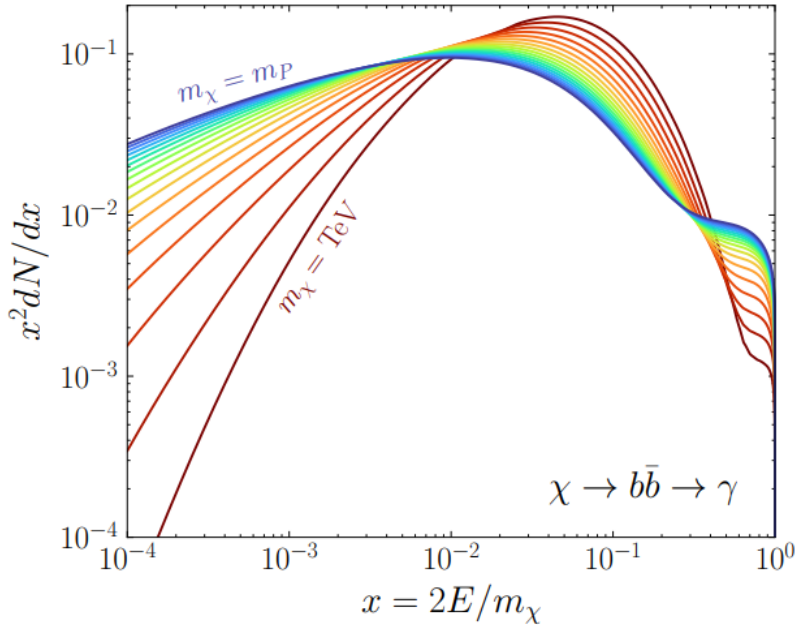


Figure 2.11 Dark Matter (DM) decay spectrum for $b\bar{b}$ initial state and γ final state. Redder spectra are for larger DM masses. Bluer spectra are light DM masses. x is a unitless factor defined as the ratio of the mass of DM, m_χ , and the final state particle energy E_γ . Figure from [19].

368 through observing galactic rotation curves. Our Milky Way galaxy is among DM dense regions
 369 discovered, and it is the largest nearby DM dense region to look at. Additionally, the DM halo
 370 surrounding the Milky Way is clumpy [18]. There are regions in the DM halo of the Milky Way that
 371 have more DM than others that have captured gas over time. These sub-halos were dense enough
 372 collapse gas and form stars. These apparent sub galaxies are known as dwarf spheroidal galaxies
 373 and are the main sources studied in this thesis. Each source type comes with different trade-offs.
 374 Galactic Center studies will be very sensitive to the assumed distribution of DM. The central DM
 375 density can vary substantially as demonstrated in Figure 2.12. At distances close to the center of
 376 the galaxy, or small r , the differences in DM densities can be 3-4 orders of magnitude. Searches
 377 toward the galactic center will therefore be quite sensitive to the assumed DM distribution.

378 Searches toward Dwarf Spheroidal Galaxies (dSph's) suffer from uncertainties in the DM
 379 density less than the galactic center studies. This is mostly from their diminutive size being smaller
 380 than the angular resolution of most γ -ray observatories [18]. The DM content dSph's are typically

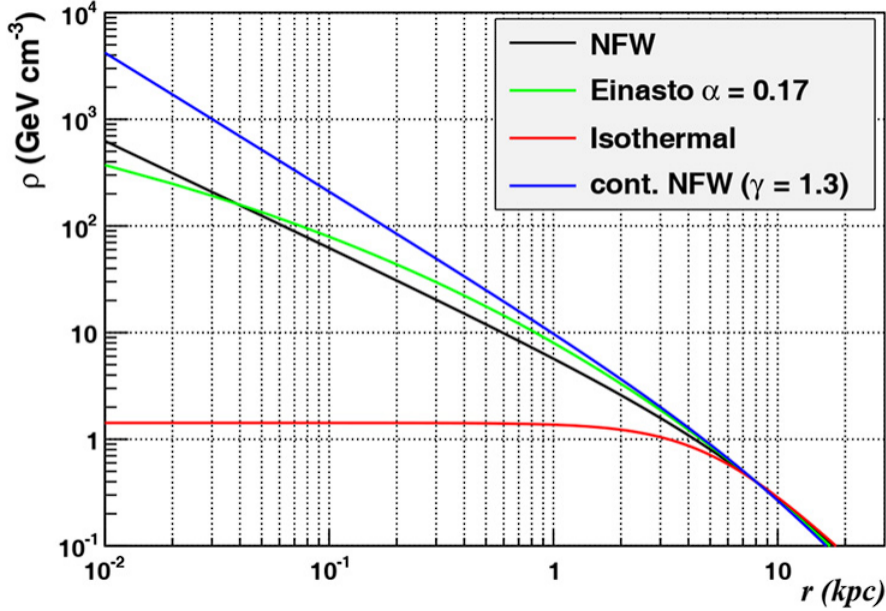


Figure 2.12 Different dark matter density profiles compared. Some models produce exceptionally large densities at small r [20].

381 determined with the Virial theorem, Equation (2.1), and are usually majority DM [18] in mass.
 382 dSph's tend to be ideal sources to look at for DM searches. Their environments are quiet with little
 383 astrophysical background. Unlike the galactic center, the most active components of dSph's are the
 384 stars within them versus a violent accretion disc around a black hole. All this together means that
 385 dSph's are among the best sources to look at for indirect DM searches. dSph's are the targets of
 386 focus for this thesis.

387 **2.6 Multi-Messenger Dark Matter**

388 Astrophysics entered a new phase in the past few decades that leverages our increasing sensitivity
 389 to SM channels and general relativity (GR). Up until the 21st century, astrophysical observations
 390 were performed with photons (γ) only. Astrophysics with this 'messenger' is fairly mature now.
 391 Novel observations of the universe have since only adjusted the sensitivity of the wavelength of
 392 light that is observed except at MeV energies. Gems like the CMB [10], and more have ultimately
 393 been observations of different wavelengths of light. Multi-messenger astrophysics proposes using
 394 other SM particles such the $p^{+/-}$, or ν or gravitation waves predicted by general relativity.

395 The experiment LIGO had a revolutionary discovery in 2016 with the first detection of a binary
 396 black hole merger [21]. This opened the collective imagination to observing the universe through
 397 gravitational waves. There has also been a surge of interest in the neutrino (ν) sector. IceCube
 398 demonstrated that we are sensitive to neutrinos in regions that correlate with significant photon
 399 emission like the galactic plane [22]. Neutrinos, like gravitational waves and light, travel mostly
 400 unimpeded from their source to our observatories. This makes pointing to the originating source
 401 of these messengers much easier than it is for cosmic rays which are deflected from their source by
 402 magnetic fields.

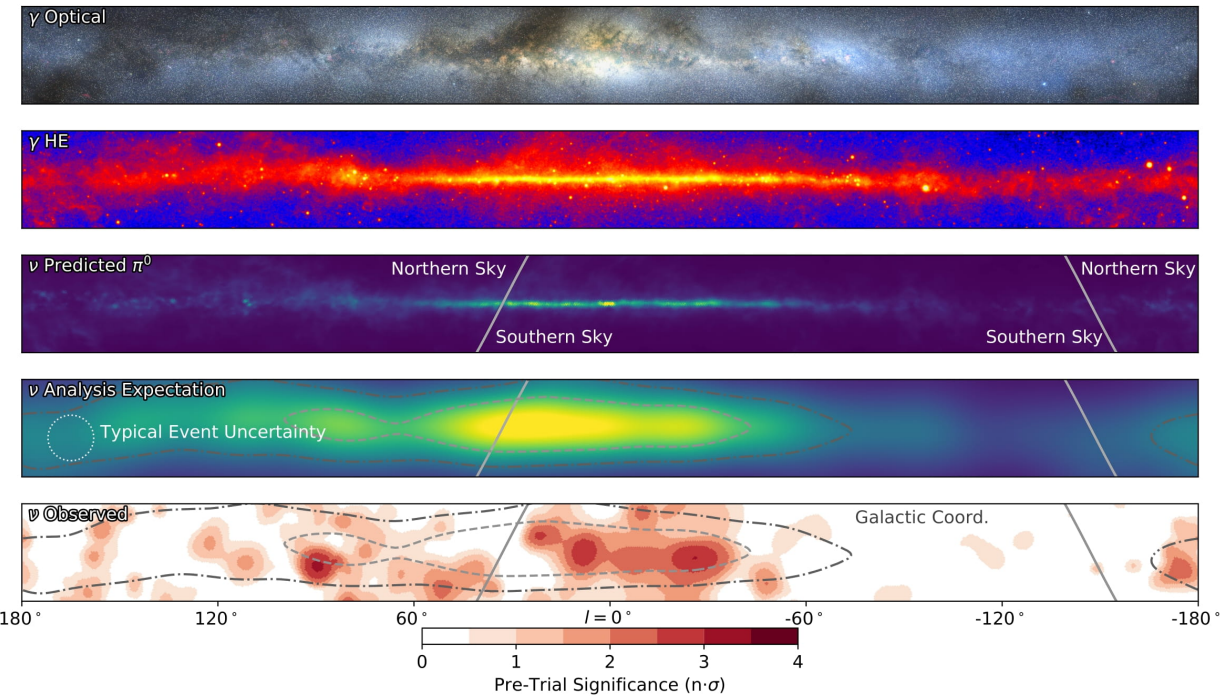


Figure 2.13 The Milky Way Galaxy in photons (γ) and neutrinos (ν) [22]. The Galactic center is at $l=0^\circ$ and is the brightest region in all panels. (top) An Optical color image of the Milky Way galaxy seen from Earth. Clouds of gas and dust obscure some light from stars. (2nd down) Integrated flux of γ -rays observed by the Fermi-LAT telescope [23]. (middle) Expected neutrino emission that corresponds with Fermi-LAT observations. (2nd up) Expected neutrino emission profile after considering detector systematics of IceCube. (bottom) Observed neutrino emission from region of the galactic plane. Substantial neutrino emission was detected.

403 The IceCube collaboration recently published a groundbreaking result of the Milky Way in
 404 neutrinos. The recent result from IceCube, shown in Figure 2.13, proves that we can make

405 observations under different messenger regimes. The top two panels show the appearance of the
 406 galactic plane to different wavelengths of light. Some sources are more apparent in some panels,
 407 while others are not. This new channel is powerful because neutrinos are readily able to penetrate
 408 through gas and dust in the Milky Way. This new image also refines our understanding of how high
 409 energy particles are produced. For example, the fit to IceCube data prefers neutrino production
 410 from the decay of π^0 [22].

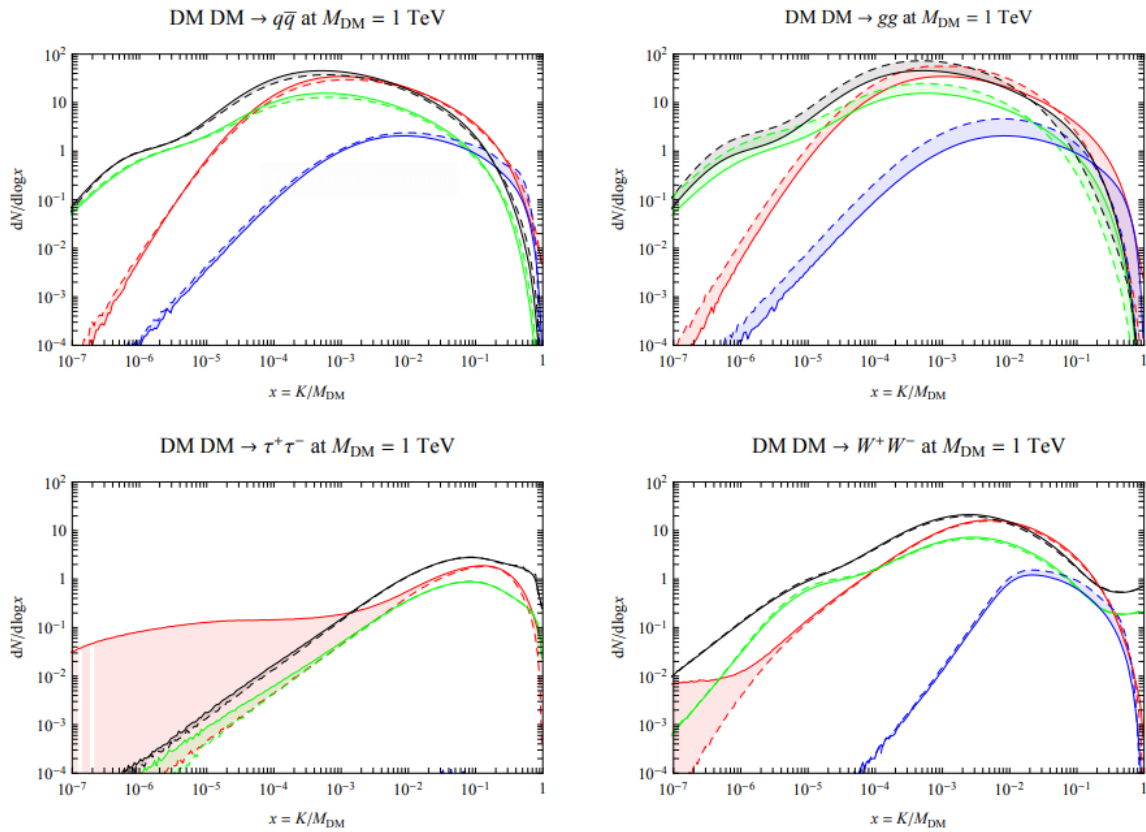


Figure 2.14 Dark Matter annihilation spectra for different final state particle and standard model annihilation channels [24]. Photons (red), e^\pm (green), \bar{p} (blue), ν (black).

411 Exposing our observations to more cosmic messengers greatly increases our sensitivity to
 412 rare processes. In the case of DM, Figure 2.14, there are many SM particles produced in DM
 413 annihilation. Among the final state fluxes are gammas and neutrinos. Charged particles are also
 414 produced however they would not likely make it to Earth since they will be deflected by magnetic

415 fields between the source and Earth. This means observatories that can see the neutral messengers

416 are especially good for DM searches and for combining data for a multi-messenger DM search.

CHAPTER 3

417 MULTIMESSENGER ASTROPHYSICS: DETECTING HIGH ENERGY NEUTRAL 418 MESSENGERS

419 3.1 Introduction

420 Before the 20th century, all asttrophysics observations were optical in nature. We litterly only
421 saw things with highly magnified optical observations. Then we discovered cosmic rays. cosmic
422 rays are charged particles, typically naked protons or H+. This was seen by Victor Hess in 19??.
423 Around the same time we discovered neutrinos from beta decay. Sometime around 1950 we started
424 to build neutrino detectors which were mostly sensitive to neutrinos from the sun. Finally, it was
425 theorized that compact objects like black holes and neutron stars would create waves in space-time
426 when they experience mergers or collisions.

427 In the 21st century, we have developed new observation techniques and detectors that are no only
428 sensitive to these four messengers - photons (TODO: photon), neutrinos (TODO: nu), Cosmic
429 Rays (CR), and Gravitational Wave (WV) - we're collect high energy versions of these events.
430 For the standad model particles, we're now sensitive to all messengers above the MeV eneryg
431 range. Additionally, the GW's were sensitive to are in the stellar mass black hole region and above
432 within our galactic neighborhood. This means were becoming sensitive to the fundamental physics
433 occuring within the universe and we can rely on the universe as a TeV+ particle accelerator. We
434 also have the abaility to correlate high energy events across messengers and gain new insights on
435 the processes that occur in our universe.

436 This thesis focuses on very high energy (VHE) gamma rays and neutrinos. These can both be
437 observed through the water cherenkov detection technique altho not exclusively. Methods on how
438 to detect and observe these neutral messengers are discussed Section 3.3 and Section 3.4

439 3.2 Charged Particles in a Medium

440 For high enery gamma-rays and neutrinos, we can exploit the same effect that charged particles
441 have with water. This effect is known as Cherenkov radiation. Cherenkov Radiation occurs when a
442 charged particle, usually electrons (e) or muons (μ), traverse a medium, like water, faster than the

443 speed of light in that medium. This is similar to sonic boom where an object moves through air
444 faster than the speed of sound in air. Cherenkov radiation can therefore be thought of as an 'optic
445 boom'. Many astro-particle physics experiments will use water as the medium as because water
446 has a unique set of properties ideal for charged particle tracking.



Figure 3.1 TODO: Show a nuclear reactor with cherenkov radiation[NEEDS A SOURCE][FACT CHECK THIS]

447 The frequency of light emitted due to cherenkov radiation follows the equation:

$$INSERTCherenkovwavelengthcalcHERE. \quad (3.1)$$

448 The absorption spectra is shown in the following figure:

449 **3.3 Photons (γ)**

450 **3.4 Neutrinos (ν)**

451 **3.5 Opportunities to Combine for Dark Matter**



Figure 3.2 TODO: absorption spectrum of liquid and solid water[NEEDS A SOURCE][FACT CHECK THIS]

CHAPTER 4

452 **HIGH ALTITUDE WATER CHERENKOV (HAWC) OBSERVATORY**

453 **4.1 The Detector**

454 **4.2 Events Reconstruction and Data Acquisition**

455 **4.2.1 G/H Discrimination**

456 **4.2.2 Angle**

457 **4.2.3 Energy**

458 **4.3 Remote Monitoring**

459 **4.3.1 ATHENA Database**

460 **4.3.2 HOMER**

461

CHAPTER 5

ICECUBE NEUTRINO OBSERVATORY

462 **5.1 The Detector**

463 **5.2 Events Reconstruction and Data Acquisition**

464 **5.2.1 Angle**

465 **5.2.2 Energy**

466 **5.3 Northern Test Site**

467 **5.3.1 PIgeon remote dark rate testing**

468 **5.3.2 Bulkhead Construction**

CHAPTER 6

COMPUTATIONAL TECHNIQUES IN PARTICLE ASTROPHYSICS

470 **6.1 Neural Networks for Gamma/Hadron Separation**

471 **6.2 Parallel Computing for Dark Matter Analyses**

472

CHAPTER 7

GLORY DUCK

473 **7.1 Data and Background**

474 **7.1.1 Data Files**

- 475 • Detector Resolution: `response_aerie_svn_27754_systematics_best_mc_test_nobroadpulse`
476 `_10pctlogchargesmearing_0.63qe_25kHzNoise_run5481_curvature0_index3.root`
- 477 • Data Map: `maps-20180119/liff/maptree_1024.root`

478 **7.1.2 Data Set Chosen**

479 The maps used for this analysis contain 1017 days of data between runs 2104 (2014-11-26) and
480 7476 (2017-12-20). They were generated from pass 4.0 reconstruction. The analysis is performed
481 using the f_{hit} energy binning scheme with bins [1-9] similar to what was done for the Crab and
482 previous HAWC dSph analysis. [25, 26].

CHAPTER 8

NU DUCK

483

BIBLIOGRAPHY

- 485 [1] Anne M. Green. “Dark matter in astrophysics/cosmology”. In: *SciPost Phys. Lect.*
 486 *Notes* (2022), p. 37. doi: [10.21468/SciPostPhysLectNotes.37](https://doi.org/10.21468/SciPostPhysLectNotes.37). URL: <https://scipost.org/10.21468/SciPostPhysLectNotes.37>.
- 488 [2] Bing-Lin Young. “A survey of dark matter and related topics in cosmology”. In: *Frontiers*
 489 *of Physics* 12 (Oct. 2016). doi: <https://doi.org/10.1007/s11467-016-0583-4>.
 490 URL: <https://doi.org/10.1007/s11467-016-0583-4>.
- 491 [3] Gianfranco Bertone, Dan Hooper, and Joseph Silk. “Particle dark matter: evidence,
 492 candidates and constraints”. In: *Physics Reports* 405.5 (2005), pp. 279–390. ISSN:
 493 0370-1573. doi: <https://doi.org/10.1016/j.physrep.2004.08.031>. URL:
 494 <https://www.sciencedirect.com/science/article/pii/S0370157304003515>.
- 495 [4] Gianfranco Bertone and Dan Hooper. “History of dark matter”. In: *Rev. Mod. Phys.*
 496 90 (4 Aug. 2018), p. 045002. doi: [10.1103/RevModPhys.90.045002](https://doi.org/10.1103/RevModPhys.90.045002). URL: <https://link.aps.org/doi/10.1103/RevModPhys.90.045002>.
- 498 [5] Fritz Zwicky. “The Redshift of Extragalactic Nebulae”. In: *Helvetica Physica Acta* 6.
 499 (1933), pp. 110–127. doi: [10.5169/seals-110267](https://doi.org/10.5169/seals-110267).
- 500 [6] Vera C. Rubin and Jr. Ford W. Kent. “Rotation of the Andromeda Nebula from a Spectro-
 501scopic Survey of Emission Regions”. In: *ApJ* 159 (Feb. 1970), p. 379. doi: [10.1086/150317](https://doi.org/10.1086/150317).
- 503 [7] K. G. Begeman, A. H. Broeils, and R. H. Sanders. “Extended rotation curves of spiral galax-
 504 ies: dark haloes and modified dynamics”. In: *Monthly Notices of the Royal Astronomical So-*
 505 *ciety* 249.3 (Apr. 1991), pp. 523–537. ISSN: 0035-8711. doi: [10.1093/mnras/249.3.523](https://doi.org/10.1093/mnras/249.3.523).
 506 eprint: <https://academic.oup.com/mnras/article-pdf/249/3/523/18160929/mnras249-0523.pdf>. URL: <https://doi.org/10.1093/mnras/249.3.523>.
- 508 [8] *Different types of gravitational lenses*. website. Feb. 2004. URL: <https://esahubble.org/images/heic0404b/>.
- 510 [9] Douglas Clowe et al. “A Direct Empirical Proof of the Existence of Dark Matter”. In: *apjl*
 511 648.2 (Sept. 2006), pp. L109–L113. doi: [10.1086/508162](https://doi.org/10.1086/508162). arXiv: [astro-ph/0608407](https://arxiv.org/abs/astro-ph/0608407)
 512 [[astro-ph](https://arxiv.org/abs/astro-ph/0608407)].
- 513 [10] Planck Collaboration and N. et. al. Aghanim. “Planck 2018 results I. Overview and the
 514 cosmological legacy of Planck”. In: *A&A* 641 (2020). doi: [10.1051/0004-6361/201833880](https://doi.org/10.1051/0004-6361/201833880). URL: <https://doi.org/10.1051/0004-6361/201833880>.
- 516 [11] Wayne Hu. *Matter Density Animation*. web. 2024. URL: <http://background.uchicago.edu/~whu/animbut/anim2.html>.

- 518 [12] Wenlong Yuan et al. “A First Look at Cepheids in a Type Ia Supernova Host with JWST”. in:
519 *The Astrophysical Journal Letters* 940.1 (Nov. 2022). doi: [10.3847/2041-8213/ac9b27](https://doi.org/10.3847/2041-8213/ac9b27).
520 URL: <https://dx.doi.org/10.3847/2041-8213/ac9b27>.
- 521 [13] Wendy L. Freedman. “Measurements of the Hubble Constant: Tensions in Perspective”. In:
522 *The Astrophysical Journal* 919.1 (Sept. 2021), p. 16. doi: [10.3847/1538-4357/ac0e95](https://doi.org/10.3847/1538-4357/ac0e95).
523 URL: <https://dx.doi.org/10.3847/1538-4357/ac0e95>.
- 524 [14] Jodi Cooley. “Dark Matter direct detection of classical WIMPs”. In: *SciPost Phys. Lect.*
525 *Notes* (2022), p. 55. doi: [10.21468/SciPostPhysLectNotes.55](https://doi.org/10.21468/SciPostPhysLectNotes.55). URL: <https://scipost.org/10.21468/SciPostPhysLectNotes.55>.
- 527 [15] “Search for new phenomena in events with an energetic jet and missing transverse momentum
528 in pp collisions at $\sqrt{s} = 13$ TeV with the ATLAS detector”. In: *Phys. Rev. D* 103
529 (11 July 2021), p. 112006. doi: [10.1103/PhysRevD.103.112006](https://doi.org/10.1103/PhysRevD.103.112006). URL: <https://link.aps.org/doi/10.1103/PhysRevD.103.112006>.
- 531 [16] *Jetting into the dark side: a precision search for dark matter*. website. July 2020. URL:
532 <https://atlas.cern/updates/briefing/precision-search-dark-matter>.
- 533 [17] Celine Armand et. al. “Combined dark matter searches towards dwarf spheroidal galaxies
534 with Fermi-LAT, HAWC, H.E.S.S., MAGIC, and VERITAS”. in: *Proceedings of Science*.
535 Vol. 395. Mar. 2022. doi: <https://doi.org/10.22323/1.395.0528>.
- 536 [18] Tracy R. Slatyer. “Les Houches Lectures on Indirect Detection of Dark Matter”. In: *SciPost*
537 *Phys. Lect. Notes* (2022), p. 53. doi: [10.21468/SciPostPhysLectNotes.53](https://doi.org/10.21468/SciPostPhysLectNotes.53). URL:
538 <https://scipost.org/10.21468/SciPostPhysLectNotes.53>.
- 539 [19] Christian W Bauer, Nicholas L. Rodd, and Bryan R. Webber. “Dark matter spectra from
540 the electroweak to the Planck scale”. In: *Journal of High Energy Physics* 2021.1029-8479
541 (June 2021). doi: [https://doi.org/10.1007/JHEP06\(2021\)121](https://doi.org/10.1007/JHEP06(2021)121).
- 542 [20] Riccardo Catena and Piero Ullio. “A novel determination of the local dark matter density”.
543 In: *Journal of Cosmology and Astroparticle Physics* 2010.08 (Aug. 2010), p. 004. doi:
544 [10.1088/1475-7516/2010/08/004](https://doi.org/10.1088/1475-7516/2010/08/004). URL: <https://dx.doi.org/10.1088/1475-7516/2010/08/004>.
- 546 [21] B. P. Abbott et al. “Observation of Gravitational Waves from a Binary Black Hole Merger”.
547 In: *Phys. Rev. Lett.* 116 (6 Feb. 2016), p. 061102. doi: [10.1103/PhysRevLett.116.061102](https://doi.org/10.1103/PhysRevLett.116.061102). URL: <https://link.aps.org/doi/10.1103/PhysRevLett.116.061102>.
- 549 [22] R. Abbasi et. al. “Observation of high-energy neutrinos from the Galactic plane”. In: *Science*
550 380.6652 (June 2023), pp. 1338–1343.

- 551 [23] NASA Goddard Space Flight Center. *Fermi's 12-year view of the gamma-ray sky*. website.
552 2022. URL: <https://svs.gsfc.nasa.gov/14090>.
- 553 [24] Marco Cirelli et al. "PPPC 4 DM ID: a poor particle physicist cookbook for dark matter
554 indirect detection". In: *Journal of Cosmology and Astroparticle Physics* 2011.03 (Mar.
555 2011), p. 051. doi: [10.1088/1475-7516/2011/03/051](https://dx.doi.org/10.1088/1475-7516/2011/03/051). URL: <https://dx.doi.org/10.1088/1475-7516/2011/03/051>.
- 557 [25] A. U. Abeysekara et al. "Observation of the Crab Nebula with the HAWC Gamma-Ray
558 Observatory". In: *The Astrophysical Journal* 843.1 (June 2017), p. 39. doi: [10.3847/1538-4357/aa7555](https://doi.org/10.3847/1538-4357/aa7555). URL: <https://doi.org/10.3847/1538-4357/aa7555>.
- 560 [26] A. Albert et al. "Dark Matter Limits from Dwarf Spheroidal Galaxies with the HAWC
561 Gamma-Ray Observatory". In: *The Astrophysical Journal* 853.2 (Feb. 2018), p. 154. ISSN:
562 1538-4357. doi: [10.3847/1538-4357/aaa6d8](https://dx.doi.org/10.3847/1538-4357/aaa6d8). URL: <http://dx.doi.org/10.3847/1538-4357/aaa6d8>.